purposes, satisfactory results are expected at temperatures up to 2,000K, which is considerably in excess of the temperature in current engineering designs.

Reference

[1]Bennett, M.D., "Velocity of Bodies Powered by Rapidly Discharged Cold-Gas Thrusters," *Journal of Spacecraft and Rockets*, Vol. 12, April 1975, pp. 254-256.

Stability of the Infrared Earth Horizon at 15μ

James William Hoffman*
Hughes Aircraft Company, El Segundo, Calif.

Introduction

FUTURE meteorological and Earth resources satellite missions involving high resolution imaging sensors will require extremely stable 3-axis attitude control systems. These systems, operating at synchronous altitude, will maintain a stable line of sight while a complete picture frame is imaged, in order to prevent picture distortion. Currently proposed systems will require an attitude reference measurement that is stable to within 1 to 2 arc sec over time periods up to 20 min long. The following experiment was performed to determine if the Earth horizon, in the 15μ region, could provide such a stable reference. If so, a simple Earth sensor could be used to provide long-term drift corrections for a gyro attitude reference system.

In this concept, the short-period attitude reference would be supplied by rate integrating gyros. The long-term attitude reference would be supplied by the horizon sensor through a very low bandwidth outer loop which smooths out the sample noise of the sensor.

Experiment Description

The method used to obtain the Earth horizon data was to utilize the video signals being telemetered to Earth from the Sun and Earth sensors aboard the Westar I Communications Satellite. Westar I is located in synchronous orbit at 99° west longitude. Although designed for another purpose, the Westar satellite provided a convenient means to conduct a preliminary investigation.

The north and south Earth sensors scan the Earth at 5° above and below the equator, with a 1.5° by 1.5° field of view, as the spacecraft spins at approximately 94 rpm. The Earth sensors are separated in spin angle (azimuth) by 45°. Each sensor employs a thermistor bolometer and a spectral filter with a 50% spectral bandpass of 13.9μ to 15.7μ. The signal is electronically filtered with a cut-on frequency of 0.5 Hz and a simple RC rolloff at 400 Hz. A typical detector has about 50 mv of noise. Both sensors are summed onto a single telemetry channel. With a 4 V signal the approximate signal to noise ratio (SNR) and single threshold position jitter (σ) caused by sensor noise alone are given by Eqs. (1) and (2).

$$\mathrm{SNR}_{\mathrm{typical}} \cong 4.0/(0.050\sqrt{2}) \cong 57 \tag{1}$$

$$\sigma \cong 1.3 \times 1.5 \text{ deg}/\mathrm{SNR} \cong 0.034 \text{ deg} \tag{2}$$

Earth horizon stability is measured by recording the time between the center of an Earth pulse and the Sun pulse and multiplying by the current angular spin velocity of the spacecraft as shown in Fig. 1.

The current value of spin velocity is obtained by measuring the time between sun pulses. To this value, correction terms are then added to account for 1) the apparent movement of the sun throughout the day θ_s; 2) the effect of orbit eccentricity on orbital rate; 3) the movement caused by Earth triaxiality acceleration θ_T; and 4) Earth parallax θ_p. Spacecraft nutation and attitude error all vary the length of the earth chord. The effect of this variation is eliminated by measuring to the center of each chord. The equations used are:

$$\epsilon_n = (T_1 + T_2)(\pi/T_s) + \theta_s + \theta_T + \theta_p \tag{3}$$

$$\theta_s = -4\pi \sum_{y=1}^{n} \left[T_{s(y)} / [T_{0(y)} - T_{s(y)}] \right] \tag{4}$$

$$T_{0(y)} = 86{,}400/[1 + 0.00044531 \cos [2\pi (t + t_0)/86{,}400]] \tag{5}$$

$$\theta_T = 2.68 \times 10^{-16} t^2 \tag{6}$$

$$\theta_p = 2.818 \times 10^{-4} \sin(\pi t_m / 43{,}200) \tag{7}$$

where T_s is instantaneous spin period of spacecraft (sec), T_0 is instantaneous orbital period of Earth (sec), t is time from start of experiment (sec), t_0 is time from orbit perigee to start of experiment (sec), and t_m is time from midnight (satellite time) (sec).

In order to make the timing circuits insensitive to long-term gain changes in the sensor, adaptive thresholding circuits were employed. These circuits set the thresholds at 50% of the pulse amplitude as measured on a previous pulse.

Results

Figures 2a and 2b show the results obtained over four separate days for the north limb and south limb, respectively. Valid data was not obtained around midnight because of the overlapping in time of the Sun and Earth pulses, which are transmitted to Earth on the same telemetry line. This interference problem (plus ground station uncertainties) could be eliminated by a dedicated experiment that employed onboard thresholding. It can be seen that at the beginning of most daily runs, a large transient occurred in the data after coming out of this interference period. These transients are most likely caused by electronic or processing effects in the experimental setup.

Before plotting, the data was smoothed by 1000 points or approximately 20 min of data (measurements were made on alternate spin cycles). A least squares regression was then performed on the data using both a 12 hour sinusoid and a 24 hour sinusoid. The 12 hour sinusoid provided the better fit and is shown (with rectangles) superimposed on the actual data. The average amplitude of the 12 hour sine wave fit for all 4 days and both sensors was 74.5 μr. The maximum change in angle for this average sinusoid over any 20 minute period is 13.0 μr as shown below in Eq. 8.

$$\Delta\theta_{\max} = 74.5\mu\mathrm{r}(2\pi/720)20 = 13.0\mu\mathrm{r} \tag{8}$$

If it is postulated that there are no significant high frequency fluctuations in the 935 km square portion of the atmosphere seen by the sensor, then this 13 μr fluctuation would represent the maximum 20 minute drift in the attitude reference.

Single threshold position jitter was computed for the data run of 23 May as a check on initial sensor accuracy estimates.

Received March 19, 1976; revision received May 3, 1976. The author wishes to acknowledge the assistance of F. Hummel, R. Eiermann, M. Hall, M. Lyon, E. Sachtleben, and B. Thomas in carrying out the experiment.

Index categories: Atmospheric, Space and Oceanographic Sciences; Earth Satellite Systems, Unmanned; Spacecraft Attitude Dynamics and Control.

*Senior Systems Engineer, Systems Laboratories, Space & Communications Group.

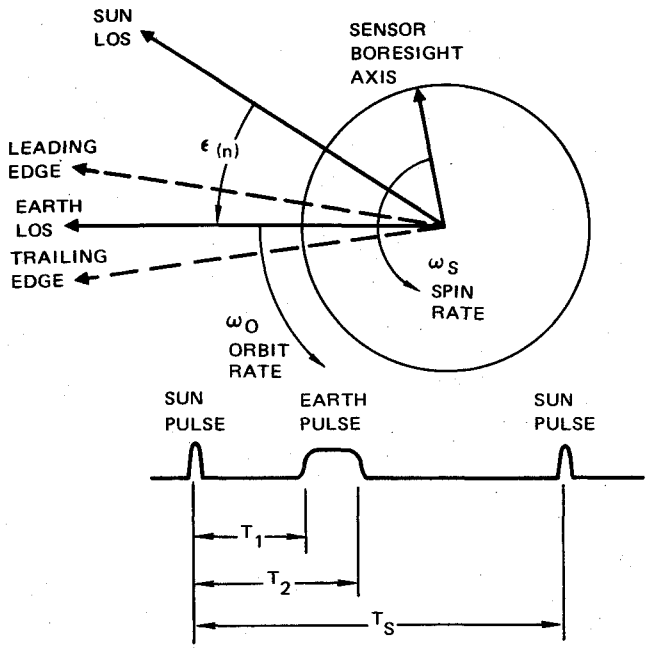

Fig. 1 Experiment geometry and waveforms

The average 1 sigma jitter for both sensors was found to be 0.0384 degrees. This value (which includes link and ground station noise) agrees well with the prediction of approximately 0.034 degrees for sensor noise alone given by Eq. 2.

Variation in Spacecraft Spin Velocity

To determine the sun to Earth angles, it was necessary to accurately determine the spin period of the spacecraft. When this spin period was plotted, an interesting 12 hour cyclic variation showed up in the data, as seen in Fig. 3. A least-square regression was then performed on the data, using a 12-hour sinusoid with an acceleration term. The resulting fit is shown with rectangles, superimposed on the smoothed data curve. The amplitude of the resulting sinusoid was 7.20 μsec or 0.00108 rpm and the spin-up rate was found to be 0.279 μsec/day. The phasing of the sinusoid shows it to peak at approximately 1:00 a.m. and 1:00 p.m. spacecraft (local) time.

An explanation for the change in spin rate can be found in the heating of the parabolic antenna about noon and midnight, the subsequent expansion of the spacecraft, and the resulting decrease in spin speed to conserve angular momentum. The Westar satellite employs a 60-in. parabolic mesh reflector for its main communications coverage. This reflector is maintained pointed at the Earth, and thus presents its maximum surface area towards the sun about noon and mid-

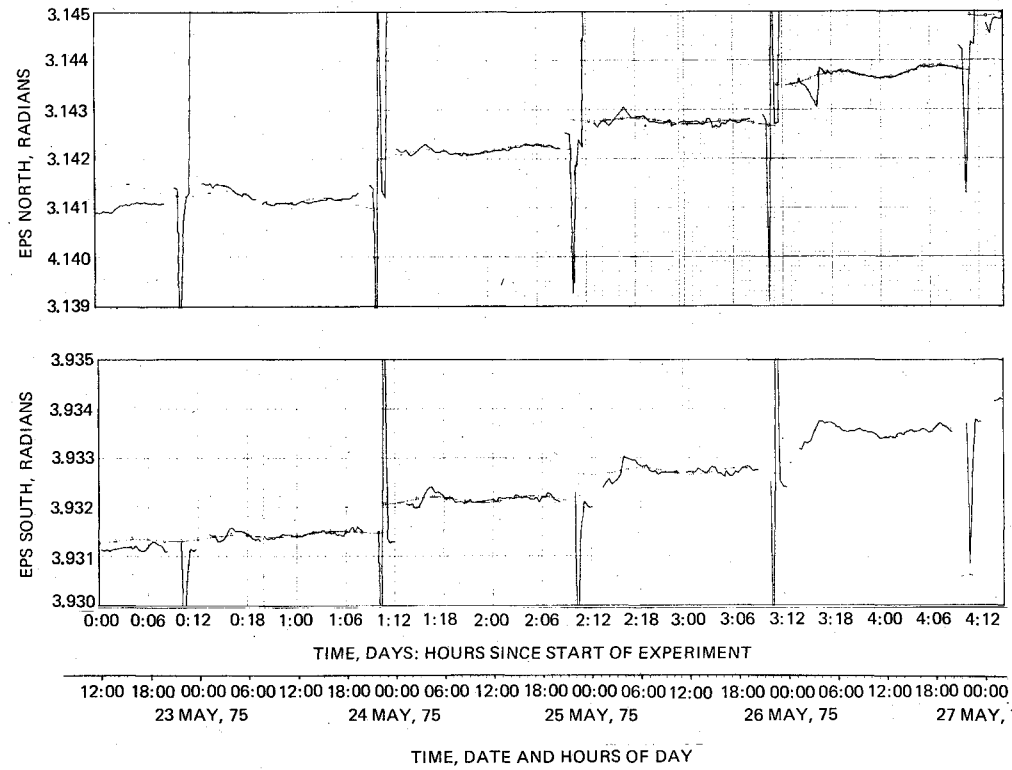

Fig. 2 North and south Earth limbs.

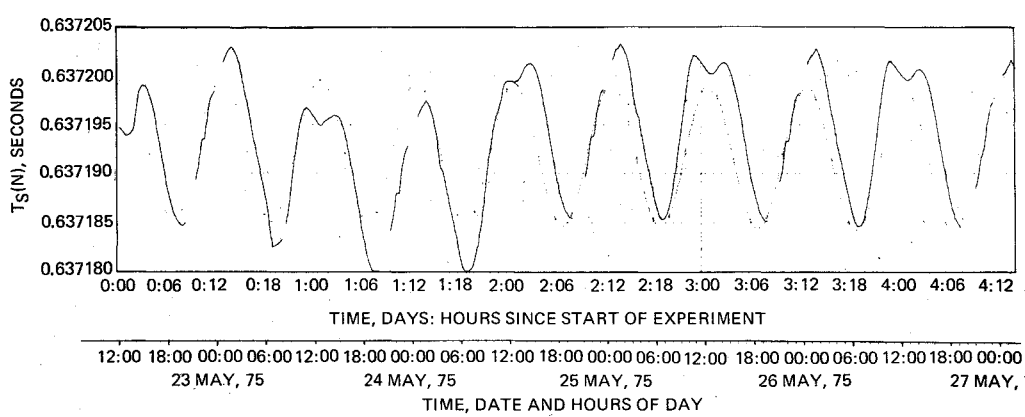

Fig. 3 Spacecraft spin period.

night, local time. The heat absorbed by the antenna is transferred through the main bearing assembly to the spinning portion of the spacecraft. Thus, at some time after noon and midnight, the spinning section reaches its maximum temperature, expands to its maximum diameter, and decreases its spin velocity to a minimum. Figure 3 shows maximum spin periods occurring at about 1:00 a.m. and 1:00 p.m., thus indicating a thermal time lag of approximately 1 hr. Telemetry measurements of Westar I solar panel temperatures, taken in early May of 1974, indicate peak-to-peak variations of about 1.1°F. Using this value and the coefficient of thermal expansion of aluminum C, the expected peak-to-peak change in spin period ΔT_s is approximately 19μsec, as shown below in Eqs. (9-11). This estimate compares favorably with the measured peak-to-peak change of 15 μsec.

$$H \simeq M \cdot R^2 . \omega \simeq 2\pi M R^2 / T_s = \text{constant} \tag{9}$$

$$R^2/T_s = (R + C \cdot \Delta T \cdot R)^2 / (T_s + \Delta T_s) \tag{10}$$

$$\Delta T_s \simeq 2C \cdot \Delta T \cdot T_s \simeq 2 \times 13.3 \times 10^{-6} \times 1.1 \times 0.636 \simeq 19 (\mu\text{sec}) \tag{11}$$

where H is angular momentum, R is radius, M is mass, and ω is angular velocity.

Conclusions

The results obtained from the experiment give some indication that the 15μ Earth horizon may be usable as a reference for ultra stable attitude control systems. Conclusive evidence would require an experiment that used 1) a sensor designed for low sample noise and good temperature stability, 2) on-board thresholding circuits that eliminate link noise, interference periods, and ground station uncertainties. Continuous data runs for longer duration could then be obtained to enable more accurate regressions and power density spectrums to be made. An additional result of interest is the semidiurnal spin speed variation caused by the thermal expansion and contraction of the spacecraft.

Noninteger Transfer Orbits for Circular Orbit Phasing Maneuvers

Gordon L. Collyer*
U.S. Army Missile Research and Development Command, Huntsville, Ala.

Nomenclature

a = semimajor axis of an elliptical orbit, ft
e = eccentricity
f = true anomaly, radians
ℓ = parameter in the polar expression for an elliptical orbit, corresponds to the radius for a true anomaly of 90°, ft
P = orbital period, sec
N = integer number of intersatellite transfer ellipses
r = radius, ft
t = transfer duration, sec
V = velocity, fps
ΔV = change in velocity, fps
λ = phase change in circular orbit, radians
θ = apsidal rotation angle, radians
μ = Earth's gravitational constant, ft^3/sec^2

Subscripts

c = circular
E = elliptical
n = nth integer transfer ellipse
R = rotation
1 = first
2 = second

Received April 5, 1976; revision received May 24, 1976.
Index categories: Earth-Orbital Trajectories; Spacecraft Mission Studies and Economics.
*Aerospace Engineer.

Introduction

A DERIVATION for optimal intersatellite transfers between locations in a given circular orbit, subject to a time limitation, is contained in Ref. 1. The transfer technique contained in that analysis involved the familiar method of using an integer number of elliptical phasing orbits, resulting in transfer opportunities only at particular times. The restriction to a discrete transfer scheme is not necessary, however, because of dynamic considerations.

A transfer technique will be developed utilizing, in general, nonintegral transfer ellipses, thereby permitting transfer opportunities as a continuous function of time. As an application, the ΔV for a simple transfer geometry will be analyzed using both the discrete and continuous methods to demonstrate an improved local minimum resulting from the continuous technique.

Transfer Technique

The transfer method presented here employs one or more elliptical transfer orbits with a burn to rotate the line of apsides provided as an additional phasing maneuver. Figure 1 depicts the transfer geometry. Note that three burns are required; the first and last burns comprising the standard Hohmann maneuver. Because the amount of apsidal rotation required becomes a function of the difference between the transfer time and the time corresponding to the last integer revolution opportunity, the geometry reduces to the discrete scheme for times corresponding to these opportunities.

First, an expression for the ΔV required by the rotation burn given the transfer time and the phase change (angular separation), will be developed. The time corresponding to the last integer revolution transfer opportunity is given from

$$t_N = P_c (N - \lambda/2\pi) \tag{1}$$

where N is the associated number of revolutions. For a transfer of specified duration the rotation of the apsidal line necessary for correct phasing becomes

$$\theta = (t - t_N) \frac{2\pi}{P_c} = 2\pi \left[\frac{t}{P_c} - \left(N - \frac{\lambda}{2\pi} \right) \right] \tag{2}$$

Given that only rotation of the apsides is desired, the true anomaly where this rotation is permitted can be found by equating the polar expressions for the orbital radii. The intersection of the orbits is as follows

$$r_1 = r_2 = \frac{\ell}{1 + e \cos(f_1)} = \frac{\ell}{1 + e \cos(f_2)} \tag{3}$$